

The diagnostic study of the plaster replicas of the Trajan's Column conserved at the Museum of Roman Civilisation (Rome)

Federica Bubola¹, Chiara Coletti¹, Eleonora Balliana², Claudia Cecamore³, Claudio Parisi Presicce³, Claudio Mazzoli¹

¹ Department of Geosciences, University of Padua, Via G. Gradenigo 6, Padua, Italy

² Department of Environmental Sciences, Informatic and Statistics, Ca' Foscari University, Via Torino 155, Mestre, Italy

³ Sovrintendenza Capitolina ai Beni Culturali, Piazza Lovatelli 35, Rome, Italy

ABSTRACT

The management of indoor microclimate in museums has recently received growing attention. Museum climatology and the mechanism for the degradation process, defined as a result of progressive and cumulative decay, depends on environmental variables and their changes. In fact, temperature and relative humidity gradients are often the main causes of chemical and physical decay of artefacts. This research focuses on assessing the state of conservation of 34 gypsum-based plaster replicas of Trajan's Column at the Museum of Roman Civilisation and on the microclimate monitoring of Room LI, where they are conserved. The decay assessment of the studied plaster casts was performed using a multidisciplinary analytical approach to characterize the constituent materials and to identify the main degradation patterns by i) on-site investigation with non-destructive methodologies; ii) chemical and petrographical characterization on collected micro samples. Microclimate variables (temperature, relative humidity and dew point) were measured along seven months to define the actual environmental conditions and the response of the materials to the microclimate.

Section: RESEARCH PAPER

Keywords: Gypsum-based plaster replicas; microclimatic monitoring; museum environment; multidisciplinary analytical approach; cultural heritage

Citation: F. Bubola, Ch. Coletti, E. Balliana, C. Cecamore, C. Parisi Presicce, C. Mazzoli, The diagnostic study of the plaster replicas of the Trajan's Column conserved at the Museum of Roman Civilisation (Rome), Acta IMEKO, vol. 13 (2024) no. 2, pp. 1-8. DOI: [10.21014/actaimeko.v13i2.1808](https://doi.org/10.21014/actaimeko.v13i2.1808)

Section Editor: Fabio Leccese, Università Degli Studi Roma Tre, Rome, Italy

Received February 27, 2024; **In final form** May 30, 2024; **Published** June 2024

Copyright: This is an open-access article distributed under the terms of the Creative Commons Attribution 3.0 License, which permits unrestricted use, distribution, and reproduction in any medium, provided the original author and source are credited.

Corresponding author: Federica Bubola, e-mail: federica.bubola@phd.unipd.it; federica.bubola@gmail.com

1. INTRODUCTION

The regulation of microclimatic conditions within museum environments and historical buildings constitutes a fundamental aspect for preserving artefacts and developing effective conservation strategies. Degradation processes, as the result of progressive and cumulative material decay, are contingent upon environmental variables and their temporal fluctuations. Specifically, suboptimal levels of temperature and relative humidity expedite chemical and physical deterioration, potentially leading to the irreversible decay of Cultural Heritage. Compared to new museums, historic buildings and archaeological sites, often lacking ideal conservation parameters, present a distinct challenge. Variations in hygrothermal conditions can induce physical and structural changes on the surface. Gypsum-based artefacts may undergo deformations,

cracks, loss of adhesion and general structural and mechanical changes, as well as solubilisation, migration and salt crystallisation. Moisture presence also influences and catalyses chemical reactions, including oxidation-reduction and hydrolysis [1]. Moreover, a high level of relative humidity and temperature fluctuations can also lead to the development of biodeteriogens. However, previous research has demonstrated that adhering to rigid temperature and relative humidity values is unnecessary. Instead, it is crucial to thoroughly understand the conservation environment and the microclimate to which the Cultural Heritage goods has adapted [2].

Although in recent years the study of plaster replicas has broadened, there are still few individual case studies that manage to fully capture the complexity of these artworks [3], [4]. Valuable information on the characterisation and the manufacture technologies of gypsum-based materials can be found in studies

on decorative stucco and mortars [5]-[9]. Nevertheless, the majority of the previous literatures prioritizes examining the physical and mechanical properties [10], [11], [12], [13], with an insight in the mineralogical composition [14], [15], [16], while research into hygroscopic properties and the interaction between the material and indoor microclimate is still relatively limited.

While gypsum typically serves as the primary material for nineteenth-century plaster replicas [17], the plaster manufacturing process often involved the addition of inorganic materials such as clays and sand, as well as organic materials such as gums and resins, to enhance mechanical properties and modify the setting time [3], [5]. Additionally, wooden and metal support structures may have been integrated during the casting process or later added during restoration interventions. Considering the multi-materiality of the plaster replicas, and that the typical decay patterns observed are often associated with environmental conditions, conducting a full characterisation of the casting materials is essential to obtain information about the deterioration processes and the relation between materials and microclimate.

This study focuses on the gypsum-based plaster replicas of Trajan's Column (113 A.D.) conserved in Room LI of the Museum of Roman Civilisation (MCR), reproducing the Trajan's military campaign to conquer Dacia. This complete set of plaster casts was produced by Pius IX for Napoleon III in 1861-1862 through the electrotyping (or galvanoplasty) process and comprises 125 casts.

Given the imminent reopening of the Museum of Roman Civilisation (the Museum has been closed since 2014) and the concurrent restoration of its plaster casts, the assessment of the current microclimate quality is crucial for the long-term preservation of these artefacts. The starting point involves the analysis of the complex interaction between microclimate dynamics and materials, focusing on evaluating the influence of temperature and relative humidity.

The following section details the materials and methods applied in the microclimatic campaign and outlines the analytical techniques employed. Section 3 presents the most significant results obtained from the analysis of the microclimate and plaster replicas. Subsequently, in the concluding section, the principal outcomes of the research are summarized.

2. MATERIALS AND METHODS

2.1. Experimental strategy

The entire collection of plaster casts reproducing the Trajan's Column has been housed in Room LI at the Museum of Roman Civilisation since around the mid-1900s, with limited information on their previous conservation status. The ongoing microclimate study enables a comparison between the current preservation state and the cast's condition in 2012, when the Museum conducted a conservation survey.

In the initial phase of the Museum's microclimate monitoring campaign, a sensor was deployed for approximately seven months, collecting climate data from November 23, 2022, to June 8, 2023, yielding a total of 4407 readings. This microclimate dataset forms the basis for understanding the environmental conditions affecting the plaster replicas.

The onsite investigation comprises the detailed analysis of 34 plaster casts, a subset of the total 125 casts reproducing the Trajan's Column. A dedicated photographic campaign documented visible degradation patterns, supporting a comprehensive decay mapping for each cast. The macroscopic

examinations were complemented using the Dino-Lite contact optical microscope, applied under natural and ultraviolet light. Additionally, InfraRed Thermography served as a valuable tool for investigating cracks and detachments in the plaster.

Two micro-samples (1-2 cm in size), A and B, were collected from the MCR_3045 plaster cast to provide insights into its material composition and degradation mechanisms. These micro-samples were analysed using different analytical methodologies: X-Ray Powder Diffraction (XRPD) for identifying mineral phases; Field Emission Scanning Electron Microscopy (FESEM) to investigate the mineralogy and morphology of the samples; Attenuated Total Reflection Infrared Spectroscopy (ATR-FTIR) for qualitative analyses of organic and inorganic compounds, and μ -Raman spectroscopy for identifying the materials constituting the plaster replicas.

The heterogeneous composition of the plaster casts and the complexity of their structure, characterized by the presence of organic and inorganic materials, underscores the necessity of employing a multi-analytical approach, complemented by a microclimatic monitoring campaign, to assess the state of conservation and the correlation between the decay patterns and the influence of temperature and relative humidity.

2.2. Microclimatic monitoring

Microclimatic monitoring was carried out using an OM-EL-USB-2LCD data logger by OMEGA®. The monitoring protocol included recording climate data at 30-minute intervals in the central area of Room LI over seven months. The sensor was set with an active alarm system based on predetermined maximum and minimum thresholds for temperature (T) and relative humidity (RH %). Specifically, the maximum temperature alarm was set at 50 °C, with a corresponding minimum temperature alarm set at -1 °C. Concerning relative humidity, the maximum alarm was triggered at a threshold of 80 %, while the minimum alarm was activated at 19.5 %.

On 17 February, the sensor was temporarily removed from the Room LI to retrieve the accumulated data. Consequently, data collected on that particular day were excluded from subsequent processing to ensure the integrity of the dataset.

The ongoing monitoring methodology has facilitated valuable data collection, essential for evaluating the microclimatic conditions within the monitored environment. Notably, this initial approach has allowed for the subsequent extension of microclimatic monitoring, involving the deployment of additional sensors strategically positioned along Room LI.

2.3. Analytical techniques

The photographs were captured using a Canon camera under 230 V 750 W halogen lamps lighting conditions. White balance adjustments were conducted in situ directly from the camera.

Thermal diffusion studies employed an InfraRed-Thermocamera (FLIR). InfraRed-images were obtained in time-lapse mode every 30 seconds (41 frames total). They were captured after heating the plaster casts with halogen lamps for 20 min at a distance of 1 m. The IR images and thermal diffusion profiles were extrapolated using FLIR ResearchIR 4 Max + HSDR software®. Images were saved in false colour using the palette GF White Hot function, in the thermal range of 11-35 °C using the FLIR system DDE (Digital Detail Enhancement) algorithm.

Diffraction data were acquired on a PANalytical X'Pert PRO diffractometer operating in Bragg-Brentano reflection geometry with CoK α radiation, 40 kV voltage, and 40 mA filament current,

equipped with an X'Celerator detector. Qualitative diffraction data analysis was carried out with X'Pert HighScore Plus® software (PANalytical) and the PDF-2 database.

Raman measurements were carried out with a Thermo Scientific DXR Raman Microscope using a 532 nm laser excitation source. Analyses were carried out using a 50x long working distance objective with ~2.5 cm spectral resolution, ~1 µm pinhole operating at 3 mW of power. Each spectrum was acquired 30 times to minimize noise with an exposure time of 1 s. Spectra were recorded in the frequency range from 100 to 3500 cm⁻¹. Spectral fitting was carried out using the Thermo Scientific OMNIC Spectra Software (Version 9) and then processed with OriginPRO 2018b.

For the Attenuated Total Reflection Infrared Spectroscopy, a Bruker ALPHA II by Bruker Optics® Fourier transform IR Spectrometer was used. ATR-FTIR analyses covered the spectral range from 4000 to 400 cm⁻¹, using a synthetic diamond crystal for sample compression. The background was measured with 48 scans before each acquisition, while the samples were analysed with 48 scans, with a resolution of 4 cm⁻¹. The spectra obtained were processed with the Thermo Scientific OMNIC Spectra Software (Version 9), and then further processed with OriginPRO 2018b.

Sample mineralogy and morphology were investigated with a FESEM Tescan Solaris. Microchemical analysis was carried out on mineral phases as observed under the FESEM using an Oxford Instrument Ultim Max 65 Silicon drift detector EDS operating at 15 keV with a current of 3 nA and a working distance of 5 mm. Backscattered electrons (BSE) were acquired to improve image resolution by working at lower tension and current (5 keV, 300 pA and at a working distance of 4 mm).

3. RESULTS AND DISCUSSION

3.1. Microclimatic monitoring

The temperature graph in Figure 1A illustrates a consistently smooth curve devoid of notable fluctuations and significant peaks, maintaining an average value of 15.06 °C. Notable temperature extremes include a minimum of 8 °C recorded on February 10, 2023 and a maximum of 26 °C documented on June 7, 2023.

In contrast, the gathered relative humidity data in Figure 1B shows a non-linear trend marked by numerous peaks and fluctuations. Daily variations in relative humidity are influenced by the day-night cycle, with a strong correlation between relative humidity and temperature. Low temperatures coincide with heightened relative humidity, especially in the early morning hours. The sensor was configured within a range from 19.5 % to 80.0 %, and instances where the relative humidity exceeded the predefined maximum level of 80 % were observed frequently. The minimum value of RH % (42 %) was recorded on the evening of March 28, 2023, while the maximum value was 86 %, recorded on January 9, 2023.

Analysing the calculated dew point data in Figure 1C reveals that the minimum dew point of 3 °C occurred on February 6, 2023, at 11 p.m., while the maximum dew point of 18.8 °C was registered on November 23, 2022, at 1 p.m.

The collected microclimatic data, displays temperature fluctuations, which, especially when combined with high humidity levels, can affect the state of conservation of the plaster replicas. Indeed, gypsum plaster, being a partially soluble material, is highly vulnerable to these fluctuations, which can lead to the formation of condensation and subsequent material

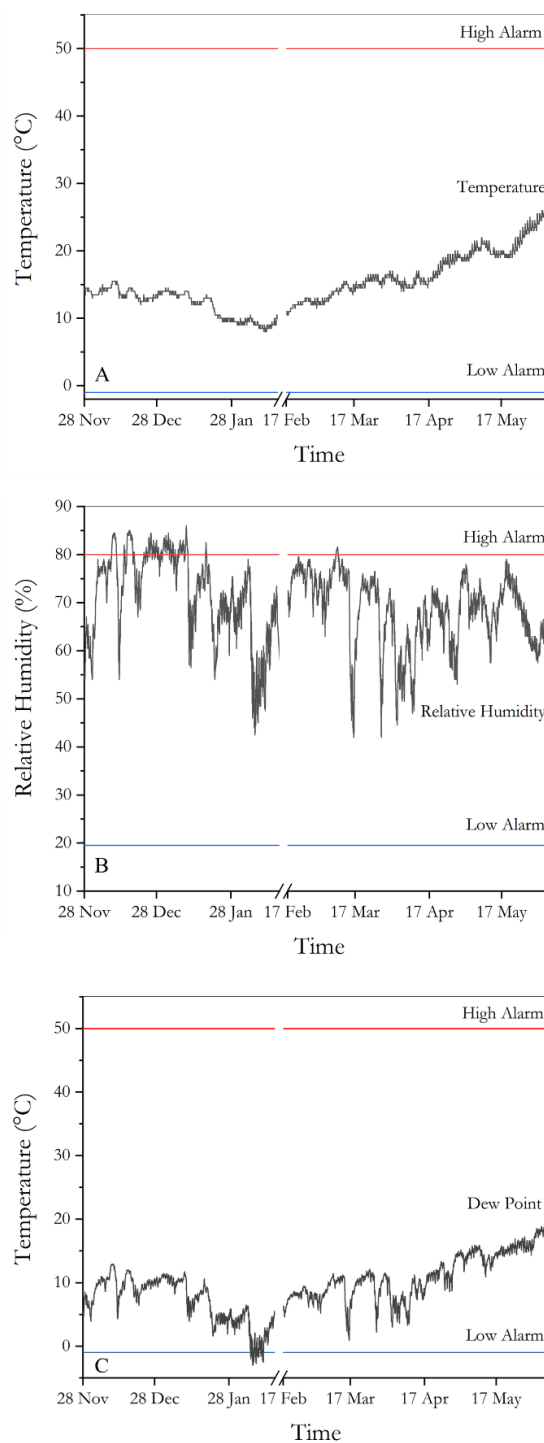


Figure 1. A) Temperature, B) Relative Humidity, and C) Dew Point data obtained from the microclimatic monitoring of Room LI over a period of seven months.

dissolution. Moreover, a high content of relative humidity can catalyse the dissolution and solubilisation of salts, resulting in recrystallisation that may cause deformations, fractures and cracks [5], [18]. This phenomenon can further increase the existing decay or even cause additional damage. The recorded temperature fluctuations from 8 °C to 26 °C suggest that decay cannot be related to freeze-thaw events, that can modify the pores connected to the environment resulting in detachment and loss of material [5], [18], [19].

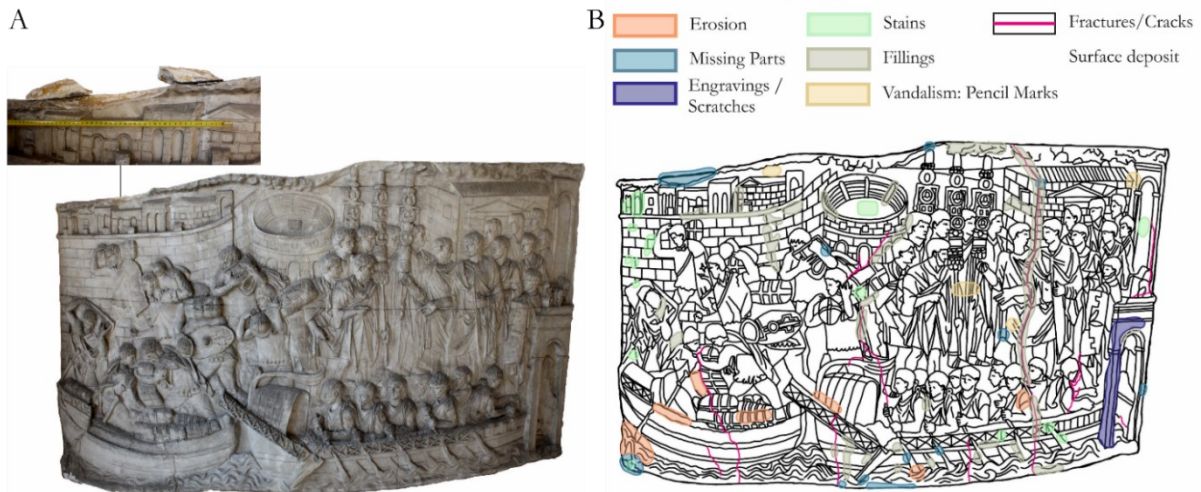


Figure 2. Plaster cast MCR_3045, with a detail of the missing part from which sample A was taken (A). Degradation map of the MCR_3045 plaster cast and the legend showing the degradation patterns (B).

3.2. In situ survey

In the conservation state survey conducted in 2012, 125 gypsum-based plaster casts were categorized into three classes based on the typology and severity of observed degradation patterns. These classes were explicitly labelled as mediocre, discreet, and poor. For this diagnostic investigation, ten plaster replicas from each class were selected for an in-depth study. Additionally, four plaster casts, not fitting any pre-defined class, were included. The selection criteria were based on institutional requirements, their preservation state, and specific Room LI location. This ensured a representative and comprehensive examination of different conservation states and conditions exhibited by the plaster casts, aligning with the objectives of the institutional conservation campaign. Most casts showed the same surface decay pattern, varying in extent and frequency/localisation.

The plaster casts consist of sections held together by a

wooden and metal structure placed on the back (Figure 3A). The structure, consists of curved, horizontal ribs covered with an irregular layer of gypsum. This complex structure of heterogeneous materials can react with the surrounding environment under very humid conservative conditions, and the presence of liquid water exacerbates this tendency, giving rise to distinct decay patterns. In presence of metallic elements within the cast, high levels of relative humidity can involve oxidation phenomena, with consequent corrosion and material expansion which can worsen scaling and detachment phenomena, leading to additional material loss also at the decorative surface [5], [18]. Notably, rust stains have been detected both on the casts' back (Figure 3A) and surface (Figure 3B).

Monitoring indoor environment is crucial in museums to safeguard artworks, which are susceptible to dust accumulation in the form of particles or fibres. Since the Museum of Roman Civilisation is closed, the primary source of dust is likely to be attributed to external factors such as road traffic and emissions

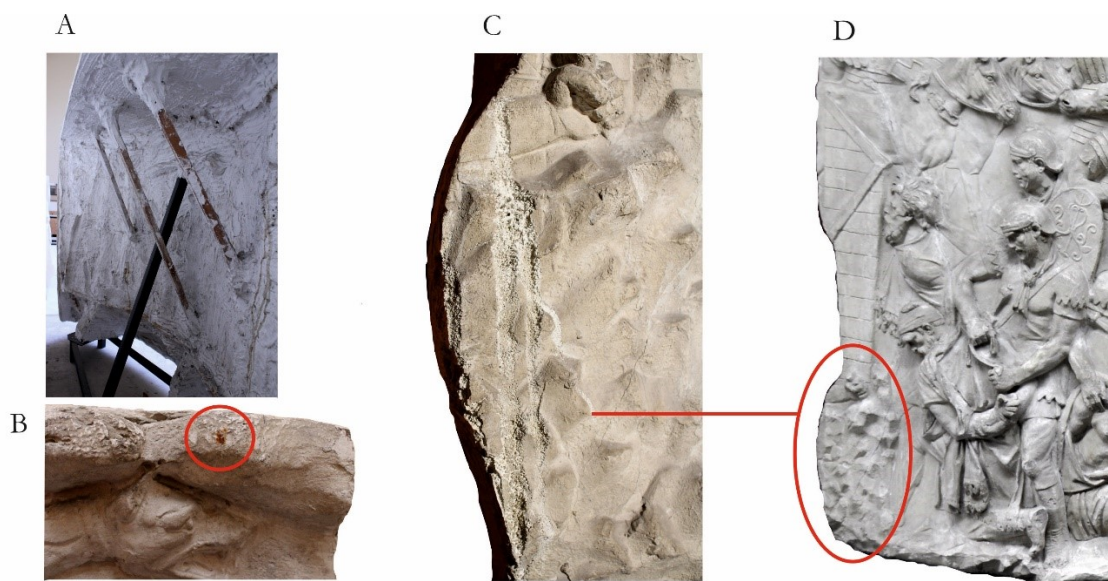


Figure 3. Detail of the wooden and metal structure placed on the back of Plaster cast MCR_3724: rust stains and drippings are visible on the irregular layer of gypsum (A). Detail of a rust stain on the surface of plaster cast MCR_3043 (B). Detail of plaster cast MCR_3052 (photo taken in 2023, during our in situ survey), which displays pulverisation as effect of the microclimate conditions (C). Detail from a photo taken during the 2012 survey of same plaster cast on Figure 2C (MCR_3052) where the material is not affected by decay patterns (D).

from industrial activities [20], [21]. Indoor conditions such as high humidity levels, can promote the adhesion of the dust to the surface [22], [23]. In general, the cast surfaces exhibit coherent deposits, especially in the most exposed areas, due to the porosity and hygroscopicity of gypsum, which primarily accounts for the tendency of this material to retain dust. Furthermore, diffuse tonal variations in yellow and pink areas are evident, likely due to historical patinas. Pencil marks are present in some areas, while scratches cover most of the cast surfaces. Each plaster cast, especially those belonging to the discreet and poor categories, shows the presence of micro-cracks and/or deep fractures, some of which extend nearly the full height of the cast. Beyond rust stains, many dark-coloured and red/brown stains of varied dimensions (up to 1-2 cm), and mortar residues are visible. These features are likely remnants from the casting process itself. Several casts exhibit regions subjected to erosion, pulverisation and lifting. Temperature and relative humidity variations can enhance weathering processes also in short time span. Photographic materials from the previous survey dated 2012 was a meaningful documentation to observe areas of erosion and pulverisation at the surface of the casts, occurred in the last decade (Figure 2C and Figure 2D). A closer examination reveals that some missing components, with surface details lost after the casts were made, subsequently required restoration efforts. Notably, these interventions are conspicuous, particularly near fractures, many coated with stucco. The fillings, discerned upon examination, exhibit varying thicknesses.

Active Infra-Red Thermography was employed to investigate the surface and subsurface features. When exposed to unsuitable environmental conditions, the artefacts can generate thermal, hygrometric and mechanical stresses, leading to alterations in the integrity of the artworks. In this regard, applying thermographic methods can provide a distinct advantage in examining surface

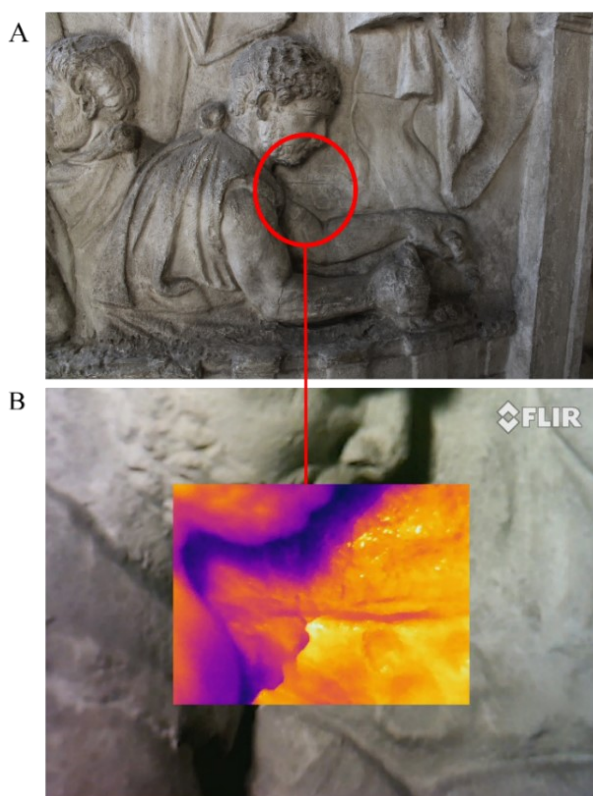


Figure 4. Detail of a fracture in the MCR_3045 plaster cast (A). Thermogram acquisition highlights the deep fracture with the uplift of the material (B).

phenomena [24]. The thermograms emphasise detachments and cracks. In Figure 4B, the area underneath, which has absorbed less heat, shows a dark colour, while the intense yellow colour highlights the more exposed surface area, since it has absorbed more heat, as it is closer to the source.

3.3. Microchemical and mineralogical characterisation

The mineralogical characterisation by XRPD analysis (Figure 5A) on the collected samples (Figure 6A) showed that the primary constituent material is gypsum (*Gp*) indicated by the presence of the characteristic diffraction pattern, with the most intense peak related to the (020) crystal plane [25], [26]. The diffractogram of sample A, collected from the bulk, shows the presence of gypsum and calcite (*Cal*) [27]. The analysis also showed traces of quartz (*Qz*) and kaolinite (*Kln*), ascribable to the manufacturing. The diffractogram of sample B, which corresponds to the surface, shows only the presence of gypsum (*Gp*) and quartz (*Qz*).

High resolution FESEM analysis allowed the study of bulk's texture and their surface and chemical analysis. The matrix of the specimen is distinguished by an elevated porosity in its bulk composition with large gypsum tabular crystals, coexisting with needle-like intermediate ones, while the surface of the sample is characterised by minerals of lower crystal size dimensions, more compactly distributed from a layer of circa 100 μm (Figure 5B). FESEM observations confirmed the XRPD data: the matrix is

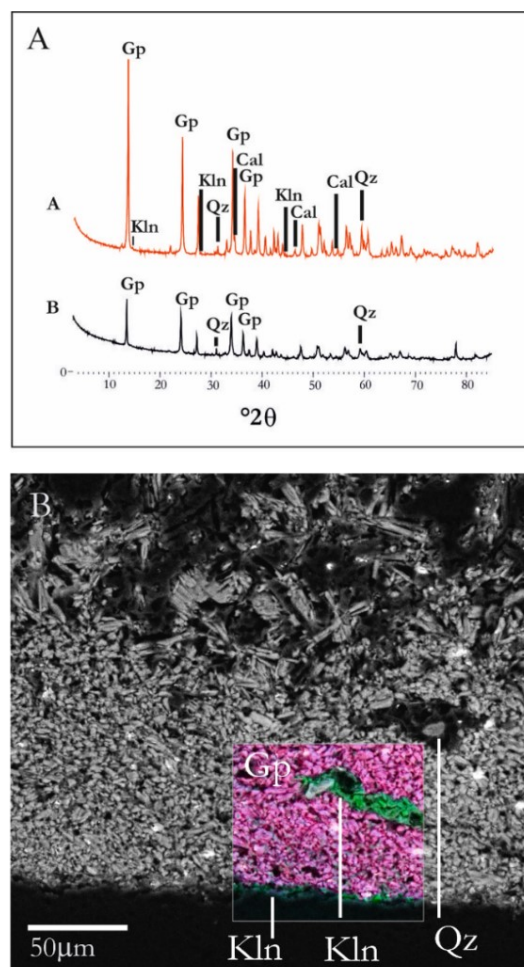


Figure 5. XRPD patterns of sample A and B (A); FESEM image of sample B. The map highlights a less porous gypsum-based matrix with inclusions of quartz and kaolinite, and a finishing rich in kaolinite (B).

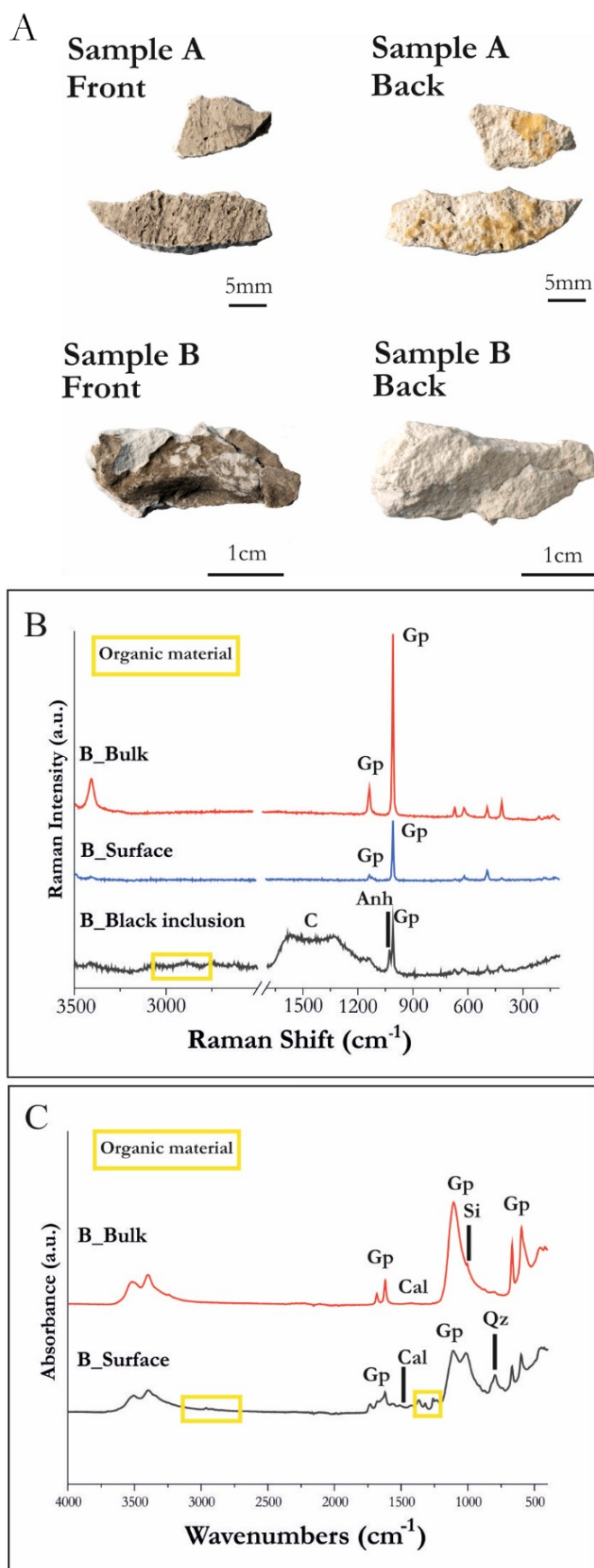


Figure 6. A) Micro-samples (Sample A and sample B, front and back) were collected from the plaster cast MCR_3045; B) Raman spectra of sample B; C) ATR-FTIR spectra of sample B.

mainly formed by gypsum crystals, with the presence of few quartz grains. EDS chemical maps on the surface area of the sample show the presence of a clayey-base coating (Figure 5B), characterised by the presence of aluminium (Al), silicon (Si) and potassium (K). Such finishing may have been applied after the moulding process. A clay finishing is indeed attested in historical recipes [28], used to change the gypsum's colour appearance and level and fill the base surfaces.

The three μ Raman spectra show the characteristic bands of gypsum at 1140, 1008, 673, 492 and 414 cm^{-1} , corresponding to the stretch vibrational mode of SO_4 (Figure 6B) [29], [30], [31], [32], [33], [34], [35], [36]. The two Raman bands observed around 3405 and 3490 cm^{-1} correspond to the O-H stretching vibration of water molecules in gypsum [32], [34]. The spectra show traces of anhydrite, with the characteristic bands of the sulphate ions at 1170, 1026 and 630 cm^{-1} [32], [34], [36]. The presence of anhydrite can be ascribed to the raw material used in the moulding of the casts [30]. μ Raman measurements did not detect the presence of calcite, given the absence of the characteristic peak at 1087 cm^{-1} [36], [37], [38]. On the other hand, amorphous carbon was detected by the narrower width and higher intensities of the characteristic bands between 1600 and 1300 cm^{-1} [33], [38].

The ATR-FTIR spectra of sample B revealed the presence of gypsum ($\text{CaSO}_4 \cdot 2\text{H}_2\text{O}$), as evidenced by the characteristic peaks at 1680, 1620 cm^{-1} (bending OH), and at 1110, 670 and 620 cm^{-1} (Figure 6C), which correspond to the stretching vibration of SO_4^{2-} , while the stretching vibrations of the water molecules within the gypsum occur at approximately 3500 and 3400 cm^{-1} [39], [40], [41], [42].

Notably, the peak at 3340 cm^{-1} in the spectrum of the surface corresponds to the stretching OH of non-bonding water molecules. The identification of the carbonate functional group, indicative of the presence of calcite, can be detected in both spectra, marked by the characteristic peaks at around 1420-1430 and 873 cm^{-1} [6], [41], [43], [44], [45]. Furthermore, the broad, low-intensity signal within the 800-770 cm^{-1} range may be attributed to quartz, either inherent in the raw material or added during the moulding process [46]. Bands at 2964, 2920, and 2850 cm^{-1} can be ascribed to the stretching CH of an organic substance, along with peaks at 1736 cm^{-1} (stretching C=O), 1562 and 1511 cm^{-1} (stretching C-C), and the bands at approximately 1370 and 1230 cm^{-1} (bending CH) [47], [48]. This organic material can be attributed to some compound used in previous interventions or as a part of a finishing application.

4. CONCLUSION

While the study of plaster replicas has expanded in recent years, few individual case studies fully capture the complexity of these materials due to their specificity. Valuable insights into gypsum-based materials' characterisation and manufacturing technologies often arise from studies on decorative stucco and mortars. However, these studies primarily focus on physical and mechanical properties, with limited research on hygroscopic properties and further research is needed to develop a deeper understanding of gypsum-based materials and their interaction within indoor environments.

The control of microclimates in museum environments or historic buildings is a fundamental aspect of protecting artefacts and planning appropriate conservation policies. Simultaneously, characterizing constituent materials and identifying primary degradation patterns through a multidisciplinary analytical

approach is essential for the long-term conservation of plaster replicas.

The microclimate data recorded between November 2023 and June 2023 show an average temperature of 15.06 °C, with relative humidity levels occasionally exceeding 80 %. Compared to the 2012 reports, it becomes evident that environmental conditions, especially fluctuations in relative humidity, have significantly impacted the preservation state of the gypsum-based plaster casts. This impact is evident due to the various forms of degradation, including new fractures, erosion, and material pulverisation. Additionally, the surfaces exhibit scratches, deposits, and stains.

The microchemical and mineralogical analyses conducted on the microsamples, have revealed that calcium sulphate dihydrate is the main component of the plaster replicas. However, traces of calcite, quartz and anhydrite have also been found. The presence of an organic material could probably derive from previous restoration interventions. In order to clarify the nature of this organic compound, the use of additional techniques such as Thermogravimetry-Differential Scanning Calorimetry and Pyrolysis Gas-Chromatography will be considered in the next future.

Ongoing analyses include on-site Hyperspectral Imaging to map and confirm forms of degradation, and colorimetric measurements to understand tonal variations on the surfaces of the plaster casts.

These results will support the restoration efforts for the plaster casts, ensuring their optimal preservation once the Museum reopens.

Furthermore, a result of a structural analysis of Room LI will be conducted using IR Thermography. Based on the results of this analysis, the microclimatic monitoring campaign will be extended, employing higher-performance sensors, strategically positioned at critical points within the gallery. The preservation of the historical gypsum replicas is of fundamental importance as evidence of the flow of time in order to preserve the memory of the evolution of the original monument.

REFERENCES

- [1] A. Spagnolo, C. Vetromile, A. Masiello, M. F. Alberghina, S. Schiavone, C. Lubritto, *Climate and Cultural Heritage: The Case Study of "Real Sito of Carditello"*, *Heritage*, vol. 2 (2019), pp. 2053-2066.
DOI: [10.3390/heritage2030124](https://doi.org/10.3390/heritage2030124)
- [2] K. Fabbri, *Historic Climate in Heritage Building and Standard 15757: Proposal for a Common Nomenclature*. *Climate*, vol. 10 (2022), pp. 4-12.
DOI: [10.3390/cli10010004](https://doi.org/10.3390/cli10010004)
- [3] V. Risdonne, C. Hubbard, J. Puieto, C. Theodorakopoulos, A multi-analytical study of historical coated plaster surfaces: the examination of a nineteenth-century V&A cast of a tombstone, *Herit. Sci.*, vol. 9 (2021).
DOI: [10.1186/s40494-021-00533-0](https://doi.org/10.1186/s40494-021-00533-0)
- [4] V. Risdonne, A. Francescutto Miró, S. Morio, C. Theodorakopoulos, *The Victoria and Albert Museum Plaster Casts by the Nineteenth-Century Workshop of the Notre-Dame Cathedral: Scientific Analysis and Conservation*, *Herit.*, vol. 5 (2022), pp. 3427-3445.
DOI: [10.3390/heritage5040176](https://doi.org/10.3390/heritage5040176)
- [5] M. Caroselli, G. Cavallo, A. Felici, S. Luppichini, G. Nicoli, L. Aliverti, G. Jean, *Gypsum in Ticinese stucco artworks of the 16-17th century: Use, characterization, provenance and induced decay phenomena*, *J. Archaeol. Sci. Rep.*, vol. 24 (2019), pp. 208-219.
DOI: [10.1016/j.jasrep.2019.01.009](https://doi.org/10.1016/j.jasrep.2019.01.009)
- [6] M. Uccelli, M. Caroselli, J. Válek, J. Zapletalová, A. Felici, G. Nicoli, G. Jean, *Characterization of the stucco decoration by Baldassarre Fontana in the Gallery of the Angels at Uherč Castle (Cz)*, *J. Archaeol. Sci. Rep.*, vol. 44 (2022), pp. 103493.
DOI: [10.1016/j.jasrep.2022.103493](https://doi.org/10.1016/j.jasrep.2022.103493)
- [7] L. Rampazzi, B. Rizzo, C. Colombo, C. Conti, M. Realini, U. Bartolucci, M. P. Colombini, A. Spiriti (+ 1 more author), *The stucco decorations from St. Lorenzo in Laino (Como, Italy): The materials and the techniques employed by the "Magistri Comacini"*, *Anal. Chem. Acta.*, vol. 630 (2008), pp. 91-100.
DOI: [10.1016/j.aca.2008.09.052](https://doi.org/10.1016/j.aca.2008.09.052)
- [8] M. Caroselli, G. Cavallo, A. Felici, L. Aliverti, S. Luppichini, G. Jean, G. Nicoli, *Characterisation of the stucco decorations at the "Sacro Monte di Ossuccio" (16th-17th century, Como, Italy)*, *Int. J. Conserv. Sci.*, vol. 7 (2016), pp. 857-870.
- [9] M. Caroselli, S. A. Ruffolo, F. Piqué, *Mortars and plasters – how to manage mortars and plasters conservation*, *Archaeol. Anthropol. Sci.*, vol. 13 (2021).
DOI: [10.1007/s12520-021-01409-x](https://doi.org/10.1007/s12520-021-01409-x)
- [10] M. T. Freie, M. do Rosário Veiga, A. Santos Silva, J. De Brito, *Restoration of ancient gypsum-based plasters: Design of compatible materials*, *Cem. Concr. Compos.*, vol. 120 (2021), pp. 104014.
DOI: [10.1016/j.cemconcomp.2021.104010](https://doi.org/10.1016/j.cemconcomp.2021.104010)
- [11] M. T. Freie, M. do Rosário Veiga, A. Santos Silva, J. De Brito, *Studies in ancient gypsum based plasters toward their repair: Physical and mechanical properties*, *Constr. Build. Mater.*, col. 202 (2019), pp. 319-331.
DOI: [10.1016/j.conbuildmat.2018.12.214](https://doi.org/10.1016/j.conbuildmat.2018.12.214)
- [12] E. Salvessa, S. Jalali, L. M. O. Sousa, L. Fernandes, A. M. Duarte, *Historical plasterwork techniques inspire new formulation*, *Constr. Build. Mater.*, vol. 48 (2013), pp. 858-867.
DOI: [10.1016/j.conbuildmat.2013.07.064](https://doi.org/10.1016/j.conbuildmat.2013.07.064)
- [13] A. Magalhães, R. Veiga, *Physical and mechanical characterisation of historic mortars. Application to the evaluation of the state of conservation*, *Mater. Constr.*, vol. 59 (2009), pp. 61-77.
DOI: [10.3989/mc.2009.41907](https://doi.org/10.3989/mc.2009.41907)
- [14] G. Gariani, P. Lehuède, L. Leroux, G. Wallez, F. Goubard, Anne Bouquillon, Marc Bormand, *First insights on the mineral composition of "Stucco" devotional reliefs from Italian Renaissance Masters: investigating technological practices and raw material sourcing*, *J. Cult. Herit.*, vol. 34 (2018), pp. 23-32.
DOI: [10.1016/j.culher.2018.05.003](https://doi.org/10.1016/j.culher.2018.05.003)
- [15] K. Elert, P. Bel-Anzué, M. Burgos-Ruiz, *Influence of calcination temperature on hydration behaviour, strength, and weathering resistance of traditional gypsum plaster*, *Constr. Build. Mater.*, vol. 367 (2023), pp. 130361.
DOI: [10.1016/j.conbuildmat.2023.130361](https://doi.org/10.1016/j.conbuildmat.2023.130361)
- [16] M. T. Freie, A. Santos Silva, M. do Rosário Veiga, J. De Brito, *Studies in ancient gypsum based plasters towards their repair: Mineralogy and microstructure*, *Constr. Build. Mater.*, vol. 196 (2019), pp. 512-529.
DOI: [10.1016/j.conbuildmat.2018.11.037](https://doi.org/10.1016/j.conbuildmat.2018.11.037)
- [17] V. Risdonne, C. Hubbard, V. H. López Borges, C. Theodorakopoulos, *Nineteenth-century Plaster Casts: a Review of Historical Sources*, *Stud. Conserv.*, vol. 67 (2022), pp. 186-208.
DOI: [10.1080/00393630.2020.1864896](https://doi.org/10.1080/00393630.2020.1864896)
- [18] E. M. Payne, *The conservation of Plaster Casts in the Nineteenth Century*, *Stud. Conserv.*, vol. 65 (2020), pp. 37-58.
DOI: [10.1080/00393630.2019.1610845](https://doi.org/10.1080/00393630.2019.1610845)
- [19] S. Salvini, C. Coletti, L. Maritan, M. Massironi, A. Pieropan, R. Spiess, C. Mazzoli, *Petrographic characterization and durability of carbonate stones used in UNESCO World Heritage Sites in northeastern Italy*, *Environ. Earth Sci.*, vol. 82 (2023), pp. 49.
DOI: [10.21203/rs.3.rs-1651027/v1](https://doi.org/10.21203/rs.3.rs-1651027/v1)
- [20] G. Battista, R. de Lieto Vollaro, *Correlation between air pollution and weather data in urban areas: Assessment of the city of Rome (Italy) as spatially and temporally independent regarding pollutants*, *Atmos. Environ.*, vol. 165 (2017), pp. 240-277.
DOI: [10.1016/j.atmosenv.2017.06.050](https://doi.org/10.1016/j.atmosenv.2017.06.050)

- [21] A. Winkler, T. Contardo, V. Lapenta, A. Sgamellotti, S. Loppi, Assessing the impact of vehicular particulate matter on cultural heritage by magnetic biomonitoring at Villa Farnesina in Rome, Italy, *Sci. Total Environ.*, vol. 823 (2022), pp. 153729. DOI: [10.1016/j.scitotenv.2022.153729](https://doi.org/10.1016/j.scitotenv.2022.153729)
- [22] A. Proietti, M. Panella, F. Leccese, E. Svezia, Dust detection and analysis in museum environment based on pattern recognition, *Meas.*, vol. 66 (2015), pp. 62-72. DOI: [10.1016/j.measurement.2015.01.019](https://doi.org/10.1016/j.measurement.2015.01.019)
- [23] A. Proietti, L. Liparulo, F. Leccese, M. Panella, Shapes classification of dust deposition using fuzzy kernel-based approaches, *Meas.*, vol. 77 (2016), pp. 344-350. DOI: [10.1016/j.measurement.2015.09.025](https://doi.org/10.1016/j.measurement.2015.09.025)
- [24] F. Mercuri, U. Zammit, N. Orazi, S. Paoloni, M. Marinelli, F. Scudieri, Active infrared thermography applied to the investigation of art and historic artefacts, *J. Therm. Anal. Calorim.*, vol. 104 (2011), pp. 475-485. DOI: [10.1007/s10973-011-1450-8](https://doi.org/10.1007/s10973-011-1450-8)
- [25] C. A. Boevens, V. V. H. Ichharam, Redetermination of the crystal structure of calcium sulphate dihydrate, $\text{CaSO}_4 \cdot 2\text{H}_2\text{O}$, *Z. Kristallogr.*, vol. 217 (2002), pp. 9-10. DOI: [10.1524/ncrs.202.217.1.9](https://doi.org/10.1524/ncrs.202.217.1.9)
- [26] L. N. Warr, IMA-CNMNC approved mineral symbols, *Mineral. Mag.*, vol. 85 (2021), pp. 291-320. DOI: [10.1180/mgm.2021.43](https://doi.org/10.1180/mgm.2021.43)
- [27] S. S. Pawelkiewicz, P. Svara, Z. Prosek, M. Keppert, E. Vejmelková, N. Murafa, T. Sawoszczuk, J. Sygula-Cholewnińska (+ 1 more author), Laboratory assessment of a photoactive Gypsum-based repair plaster, *constr. Build. Mater.*, vol. 346 (2022), pp. 128426. DOI: [10.1016/j.conbuildmat.2022.128426](https://doi.org/10.1016/j.conbuildmat.2022.128426)
- [28] T. Turco, Il gesso lavorazione – trasformazione – impieghi, Ulrico Hoepli, Milano, 1861, BID: SBL0247741, BNI616859. [In Italian]
- [29] V. Antunes, A. Candeias, M. J. Oliveira, S. Longelin, V. Serrão, A. I. Seruya, J. Coroado, L. Dias, (+ 2 more authors), Characterization of gypsum and snhydrite ground layers in 15th and 16th centuries Portuguese paintings by Raman Spectroscopy and other techniques, *J. Raman Spectrosc.*, vol. 45 (2014), pp. 1026-1033. DOI: [10.1002/jrs.4488](https://doi.org/10.1002/jrs.4488)
- [30] N. Prieto-Taboada, O. Gómez-Laserna, I. Martínez-Arkarazo, M. A. Olazabal, J. M. Madariaga, Raman Spectra of the Different Phases in the $\text{CaSO}_4 \cdot \text{H}_2\text{O}$ System, *Anal. Chem.*, vol. 86 (2014), pp. 10131-10137. DOI: [10.1021/ac501932f](https://doi.org/10.1021/ac501932f)
- [31] H. G. M. Edwards, M. T. Doménech-Carbó, M. D. Hargreaves, A. Doménech-Carbó, A Raman spectroscopic and combined analytical approach to the restoration of severely damaged frescoes: the Palomino project, *J. Raman Spectrosc.*, vol. 39 (2008), pp. 444-452. DOI: [10.1002/jrs.1854](https://doi.org/10.1002/jrs.1854)
- [32] T. Schmid, P. Dariz, Chemical imaging of historical mortars by Raman microscopy, *Constr Build Mater.*, vol. 114 (2016), pp. 506-516. DOI: [10.1016/j.conbuildmat.2016.03.153](https://doi.org/10.1016/j.conbuildmat.2016.03.153)
- [33] I. Martínez-Arkarazo, D. C. Smith, O. Zuloaga, M. A. Olazabal, J. M. Madariaga, Evaluation of three different mobile Raman microscopes employed to study deteriorated civil building stones, *J. Raman Spectrosc.*, vol. 39 (2008), pp. 1018-1029. DOI: [10.1002/jrs.1941](https://doi.org/10.1002/jrs.1941)
- [34] P. S. R. Prasad, A. Pradhan, T. N. Gowd, *In situ* micro-Raman investigation of dehydration mechanism in natural gypsum, *Curr. Sci.*, vol. 80 (2001), pp. 1203-1207.
- [35] H. G. M. Edwards, S. E. J. Villar, J. Parnell, C. S. Cockell, P. Lee, Raman spectroscopic analysis of cyanobacterial gypsum halotrophs and relevance for sulfate deposits on Mars, *R. Soc. Chem.*, vol. 130 (2005), pp. 917-923. DOI: [10.1039/b503533c](https://doi.org/10.1039/b503533c)
- [36] A. Sarmiento, M. maguregui, I. Martinez-Arkazo, M. Angulo, K. Castro, M. A. Olazábal, L. A. Fernández, M. D. Rodríguez-Laso (+ 3 more authors), Raman spectroscopy as a tool to diagnose the impacts of combustion and greenhouse acid gases on properties of Built Heritage, *J. Raman Spectrosc.* Vol. 39 (2008), pp. 1042-1049. DOI: [10.1002/jrs.1937](https://doi.org/10.1002/jrs.1937)
- [37] D. Seol, Y. Ma, K. Nam, H. Chung, A study on Raman spectroscopic scheme enabling fast and accurate determination of calcite concentration in gypsum, *Microchem. J.*, vol. 172 (2021), pp. 240-252. DOI: [10.1016/j.chemgeo.2008.11.008](https://doi.org/10.1016/j.chemgeo.2008.11.008)
- [38] S. E. Spoto, G. Paladini, F. Caridi, V. Crupi, S. D'Amico, D. Majolino, V. Venuti, Multi-Technique Diagnostic Analysis of Plaster Mortars from the *Church of the Annunciation* (Tortorici, Sicily), *Mater.*, vol. 15 (2022), pp. 958-972. DOI: [10.3390/ma15030958](https://doi.org/10.3390/ma15030958)
- [39] D. Gramtorp, K. Botfeldt, J. Glastrup, K. P. Simonsen, Investigation of Anne Marie Carl-Nielsen's wax models, *Stud. Conserv.*, vol. 60 (2015), pp. 97-106. DOI: [10.1179/2047058413y/0000000111](https://doi.org/10.1179/2047058413y/0000000111)
- [40] G. Vasco, A. Serra, D. Manno, G. Buccolieri, L. Calcagnile, L. Miotto, L. Valli, A. Buccolieri, Diagnostic investigation to support the restoration of the polychrome terracotta relief "*Madonna and Child*" in Piove di Sacco (Padova, Italy), *J. Cult. Herit.*, vol. 53 (2021), pp. 80-87. DOI: [10.1016/j.culher.2021.11.009](https://doi.org/10.1016/j.culher.2021.11.009)
- [41] G-L. Liu, S. G. Kazarian, Recent advances and applications to cultural heritage using ATR-FTIR spectroscopy and ATR-FTIR spectroscopic imaging, *R. Soc. Chem.*, vol. 147 (2022), pp. 1777-1797. DOI: [10.1039/d2an00005a](https://doi.org/10.1039/d2an00005a)
- [42] L. Bishop, M. D. Dyar, S. J. King, A. J. Brown, G. A. Swayze, What Lurks in the Martian Rocks and Soil? Investigation of Sulfates, Phosphates, and Perchlorates. Spectral properties of Ca-sulfates: Gypsum, bassanite and anhydrite, *Am. Mineral.*, vol. 99 (2014), pp. 2105-2115. DOI: [10.2138/am-2014-4756](https://doi.org/10.2138/am-2014-4756)
- [43] F. A. Andersen, L. Brečević, Infrared Spectra of Amorphous and Crystalline Calcium Carbonate, *Acta Chem. Scand.*, vol. 45 (1991), pp. 1018-1024. DOI: [10.389/acta.chem.scand.45-1018](https://doi.org/10.389/acta.chem.scand.45-1018)
- [44] T. Lamhasni, H. El-Marjaoui, A. El Bakkali, S. Ait Lyazidi, M. Haddad, A. Be-Ncer, F. Benyaich, A. Bonazza (+ 1 more author), Air pollution impact on architectural heritage of Morocco: Combination of synchronous fluorescence and ATR-FTIR spectroscopies for the analyses of black crusts deposits, *Chemosphere*, vol. 225 (2019), pp. 517-523. DOI: [10.1016/j.chemosphere.2019.03.109](https://doi.org/10.1016/j.chemosphere.2019.03.109)
- [45] M. M. Jordán, J. Jordá, F. Pardo, M. A. Montero, Mineralogical Analysis of Historical Mortars by FTIR, *Mater.*, vol. 12 (2018), pp. 55-59. DOI: [10.3390/ma12010055](https://doi.org/10.3390/ma12010055)
- [46] I. Fikri, M. El Amraoui, M. Haddad, A. S. Ettahiri, C. Falguères, L. Bellot-Gurlet, T. Lamhasni, S. A. Lyazidi, (+ 1 more author), Raman and ATR-FTIR analyses of medieval wall paintings from al-Qaeaqiyyin in Fez (Morocco), *SAA*, vol. 280 (2022), pp. 121557. DOI: [10.1016/j.saa.2022.121557](https://doi.org/10.1016/j.saa.2022.121557)
- [47] F. Pozzi, E. Basso, S. Alderson, J. Levinson, M. Neimar, S. Alcalá, Aiding the cleaning of four 19th-century Tsimshian house posts: investigation of museum-applied surface coatings and original polychromy, *Herit. Sci.*, vol. 9 (2021), pp. 42-59. DOI: [10.1186/s40494-021-00513-4](https://doi.org/10.1186/s40494-021-00513-4)
- [48] V. Guglielmi, C. A. Lombardi, G. Fiocco, V. Comite, A. Bergomi, M. Borelli, M. Azzarone, M. Malagodi (+ 2 more authors), Multi-Analytical Investigation on Renaissance Polychrome Earthenware Attributed to Giovanni Antonio Amedeo, *Appl. Sci.*, vol. 13 (2023), pp. 3924. DOI: [10.3390/app13063924](https://doi.org/10.3390/app13063924)